Catastrophic Drought in the Afro-Asian Monsoon Region During Heinrich Event 1

J. Curt Stager, *et al.*

Science **331**, 1299 (2011);
DOI: 10.1126/science.1198322

reason, the SOA observed in polluted air cannot be unambiguously attributed to formation from SVOCs and IVOCs. The DWH oil spill provided a unique look at this chemistry because the emissions of VOCs, IVOCs, and SVOCs were spatially separated and the importance of SOA formation from IVOCs could be clearly demonstrated. These results form a well-constrained case to improve our quantitative understanding of IVOC chemistry, which will help to describe the importance of IVOCs for SOA formation in other polluted regions of the atmosphere.

References and Notes

1. T. J. Crone, M. Tolstoy, *Science* **330**, 634 (2010); 10.1126/science.1195840.
2. See supporting material on *Science* Online.
3. M. Kanakidou *et al.*, *Atmos. Chem. Phys.* **5**, 1053 (2005).
4. T. B. Ryerson *et al.*, *Geophys. Res. Lett.* 10.1029/2011GL046726 (2011).
5. Q. Zhang *et al.*, *Geophys. Res. Lett.* **34**, L13801 (2007).
6. J. de Gouw, J. L. Jimenez, *Environ. Sci. Technol.* **43**, 7614 (2009).
7. A. L. Robinson *et al.*, *Science* **315**, 1259 (2007).
8. J. A. de Gouw *et al.*, *J. Geophys. Res.* **110**, D16305 (2005).
9. R. Volkamer *et al.*, *Geophys. Res. Lett.* **33**, L17811 (2006).
10. H. Matsui *et al.*, *J. Geophys. Res.* **114**, D04201 (2009).
11. D. Johnson *et al.*, *Atmos. Chem. Phys.* **6**, 403 (2006).
12. N. M. Donahue, A. L. Robinson, S. N. Pandis, *Atmos. Environ.* **43**, 94 (2009).
13. NOAA-NESDIS, Satellite Derived Surface Oil Analysis Products—Deepwater Horizon (www.ssd.noaa.gov/PS/MPS/deepwater.html).
14. Spill Related Properties of MC 252 Crude Oil Sample ENT-052210-178, SL Ross Environmental Research Ltd. for British Petroleum (July 2010); see www.restorethegulf.gov/sites/default/files/documents/pdf/OilBudgetCalc_Full_HQ-Print_111110.pdf, Appendix 8.
15. D. V. Spracklen, S. R. Arnold, J. Sciare, K. S. Carslaw, C. Pio, *Geophys. Res. Lett.* **35**, L12811 (2008).
16. N. L. Ng *et al.*, *Atmos. Chem. Phys.* **7**, 3909 (2007).
17. C. E. Jordan *et al.*, *Atmos. Environ.* **42**, 8015 (2008).
18. A. K. Baker *et al.*, *Atmos. Environ.* **42**, 170 (2008).
19. C. Warneke *et al.*, *J. Geophys. Res.* **112**, D10S47 (2007).
20. F. Counillon, L. Bertino, *Ocean Dyn.* **59**, 83 (2009).
21. E. P. Chassignet *et al.*, *Oceanography* **22**, 64 (2009).
22. W. H. White *et al.*, *Science* **194**, 187 (1976).

23. We thank the flight crew of the NOAA WP-3D, as well as NOAA's National Environmental Satellite, Data, and Information Service, for the oil spill maps in Fig. 1. Supported by the NASA Radiation Sciences Program (D.W.F., A.E.P., J.P.S., J.R.S., and L.A.W.), NSF grant 1048697 (C.P., M.L.H., and A.S.) and a U.S. Coast Guard Pollution Removal Funding Authorization to NOAA for flights over the oil spill made by the NOAA WP-3D.

Supporting Online Material

www.sciencemag.org/cgi/content/full/331/6022/1295/DC1
Materials and Methods
Figs. S1 to S3
References

11 November 2010; accepted 3 February 2011
10.1126/science.1200320

Catastrophic Drought in the Afro-Asian Monsoon Region During Heinrich Event 1

J. Curt Stager,[1,2]* David B. Ryves,[3] Brian M. Chase,[4,5] Francesco S. R. Pausata[6,7,8]

Between 15,000 and 18,000 years ago, large amounts of ice and meltwater entered the North Atlantic during Heinrich stadial 1. This caused substantial regional cooling, but major climatic impacts also occurred in the tropics. Here, we demonstrate that the height of this stadial, about 16,000 to 17,000 years ago (Heinrich event 1), coincided with one of the most extreme and widespread megadroughts of the past 50,000 years or more in the Afro-Asian monsoon region, with potentially serious consequences for Paleolithic cultures. Late Quaternary tropical drying commonly is attributed to southward drift of the intertropical convergence zone, but the broad geographic range of the Heinrich event 1 megadrought suggests that severe, systemic weakening of Afro-Asian rainfall systems also occurred, probably in response to sea surface cooling.

Meridional repositioning of the intertropical convergence zone (ITCZ), the primary source of rainfall in most of the tropics, is thought to have been a major source of hydrological variability during the late Quaternary (*1*–*4*). For example, ice sheet expansion forced the mean latitudinal position of the ITCZ southward along with other atmospheric circulation systems in the Northern Hemisphere during the Last Glacial Maximum (*3*), and abrupt North Atlantic cooling during deglacial melting and ice-rafting episodes such as Heinrich stadial 1 (HS-1), along with associated reductions of marine meridional overturning circulation (MOC), is also thought to have had a similar effect on rain belts associated with the ITCZ (*1*, *3*, *4*). Some model simulations of Northern Hemisphere climatic changes associated with HS-1 indicate a southward drift of up to 10 latitudinal degrees (*2*). Most of northern Africa became unusually dry around 16 to 17 thousand calendar years ago (ka) during the HS-1 ice-rafting peak of Heinrich event 1 (H1), including the Sahara and Sahel (*5*), Ethiopia (*6*), and the Red Sea region (*7*), as did most of southern Asia (*8*–*11*) (Figs. 1 and 2). Affecting most of the northern Old World tropics, this arid episode brought some of the most severe drought conditions of the past 50,000 years or more to many of the terrestrial sites that cover such long time periods in detail (Fig. 2 and SOM Text).

Under such circumstances, a more southerly positioned ITCZ would presumably deliver less rain to the northern tropics while causing little change near the equator and wetter conditions in the southern tropics. However, a relative scarcity of high-resolution paleoclimate records from much of the inner and southern tropics has left this commonly cited hypothesis sparsely tested, particularly in Africa. This, in turn, has also limited understanding of the effects of major events such as H1 on global climates. We present a collection of new and recently published records from Africa that register severe aridity in the equatorial and southern tropics about 16 to 17 ka, thereby showing that the H1 megadrought extended far beyond the northern tropics and was therefore one of the most intense and far-reaching dry periods in the history of anatomically modern humans. Together, these records also show that southward drift of the ITCZ cannot have been the only cause of low-latitude drought during H1, and instead suggest that a substantial weakening of tropical rainfall systems also occurred.

If the ITCZ did shift several degrees southward over Africa and Asia during H1, it should still have delivered rains to equatorial regions once or twice annually unless the latitudinal shift was unrealistically large, on the order of 20° or more. However, extreme equatorial drying centered on 16 to 17 ka also occurred in northern Tanzania [(*12*) and this study], Ghana (*13*), and the Niger-Sanaga and Congo watersheds (*14*, *15*) (Fig. 1), as well as in Borneo on the opposite side of the Indian Ocean (*16*), much as it did in the more northerly reaches of the tropics from the Mediterranean Basin to the western Pacific (Figs. 1 to 3 and SOM Text).

A dramatic event associated with these equatorial changes was the desiccation of Lake Victoria, East Africa (Fig. 1), which today is the world's largest tropical lake. With rainfall over the watershed possibly reduced to less than a quarter of its present amount (*7*), the lake dried out twice between 15 and 18 ka, although the timing of the two low stands has previously been unclear (SOM Text). We present here radiocarbon dates and diatom records from two cores, which show that the first of these low stands occurred about 16 to 17 ka (Fig. 3D) (*17*). The disappearance of Lake Victoria would have had severe ecological impacts on regional ecosystems and cultures from

[1]Natural Sciences, Paul Smith's College, Paul Smiths, NY 12970, USA. [2]Climate Change Institute, University of Maine, Orono, ME 04469, USA. [3]Centre for Hydrological and Ecosystem Science, Department of Geography, Loughborough University, Loughborough, LE11 3TU, UK. [4]Institut des Sciences de l'Evolution de Montpellier, UMR 5554 Université Montpellier 2, Bâtiment 22, CC061, Place Eugène Bataillon 34095 Montpellier CEDEX 5, France. [5]Department of Archaeology, History, Cultural Studies and Religion, University of Bergen, 5020 Bergen, Norway. [6]Geophysical Institute, University of Bergen, Allégaten 70, 5007 Bergen, Norway. [7]Bjerknes Centre for Climate Research, Allégaten 55, 5007 Bergen, Norway. [8]European Commission, Joint Research Centre, Institute for Environment and Sustainability, Climate Change Unit, Ispra, Italy.

*To whom correspondence should be addressed. E-mail: cstager@paulsmiths.edu

eastern equatorial Africa to the Mediterranean coast. It is the largest water source for the Nile River during seasonal low-flood stages, and Lake Tana, Ethiopia, is the primary source of the Nile's seasonal high floods; both lakes dried out completely at that time (*6*).

In addition, an analysis of diatom assemblages in a core from Lake Tanganyika, Tanzania (*17*), supports geochemical evidence (*18*) that a major low stand occurred about 16 to 17 ka there, as well (Figs. 2D and 3F). We therefore link the synchronous regressions at Lakes Victoria and Tanganyika to the H1 ice-rafting peak that occurred about 16 to 17 ka during the longer Heinrich stadial period in the North Atlantic (*3*, *19*), while recognizing that the ages assigned to these events are subject to the limitations of radiocarbon dating, variable carbon reservoir effects, and bioturbation. Together, these equatorial records demonstrate that a simple southward shift of the ITCZ cannot have been the only climatic mechanism to affect tropical rainfall substantially during H1.

The occurrence of major droughts to the south of equatorial Africa during H1 even more clearly requires a mechanism other than southward drift of the ITCZ over the continent, which would be expected to make those regions wetter as the north became drier (Figs. 1 to 3). These sites included Lake Malawi (*20*), the Zambezi and Limpopo watersheds (*21*, *22*), and other locations in southeastern Africa (Fig. 1 and SOM Text).

In contrast, parts of southwestern Africa became wetter during H1 (*23*), but hydrology there can also be influenced by rainfall systems other than the ITCZ, such as winter storms carried on the austral mid-latitude westerlies. The complexity of the interactions between subtropical and Southern Ocean dynamics is highlighted in a stable isotope record from the Western Cape, where changes in sea surface temperatures (SST) as a result of variability in MOC and/or the Agulhas Current caused progressively wetter conditions in that region across H1 (*24*) (Fig. 1). Further north, in the Kalahari, Burrough *et al*. (*25*) favored an easterly ITCZ rainfall source for the enlarged paleolake Makgadikgadi, proposed largely on the basis of sandy deposits on western shorelines, but droughts to the north and east, along with the possibility of distant runoff sources in addition to deflation and downwind sediment deposition during dry seasons, suggest an alternative interpretation as well. Wetter conditions in the Kalahari at that time might also be consistent with a northward extension of winter rains, which could have brought increased precipitation to Namibia during H1 (*26*). Wetter conditions could also reflect enhanced runoff from high stratiform clouds and fogs in the Angola highlands related to cooling along the Benguela coast (*27*), rather than a southward shift of the ITCZ alone.

Hydrological conditions in the New World tropics are difficult to interpret in this context. Extreme aridity is registered in cores from the Cariaco Basin about 16 to 17 ka (*1*), and regional increases in precipitation occurred farther south in the tropical Andes and parts of Amazonia during H1 (*1*, *3*). This pattern appears to be consistent with a southward shift of the mean position of the ITCZ, although it is not found universally (SOM Text). Most important in the context of this study, however, the development of wet conditions in numerous neotropical sites suggests that the proposed general weakening of rainfall systems over Africa did not occur in South America and that it apparently represented regional, rather than uniformly global, changes in tropical atmospheric circulation.

General circulation models (GCMs) often have more difficulty in simulating precipitation than temperature, and GCM reconstructions of tropical rainfall are less well supported by historical instrumental weather data than those that focus on the northern temperate zone. Furthermore, to our knowledge, no modeling studies of deglacial climates have as yet been constrained by a detailed array of paleohydrological records spanning most of the African continent. Our findings are therefore useful for evaluating model reconstructions of past climates in Africa and of the global effects of H1, and we summarize several GCM simulations here to illustrate the difficulty of reconciling current GCM output with paleoclimatic reconstructions. For example, although Mulitza *et al*. (*5*) correctly simulated Sahel aridity in response to weakened MOC that was typical of the HS-1 interval, the model shows wetting over much of central Africa that is inconsistent with the data available. Kageyama *et al*. (*2*) correctly inferred Indian aridity but did not fully extend it to equatorial and southern Africa, whereas simulations by Thomas *et al*. (*4*), which identified wetting in the Angola-Kalahari region, did not completely capture the extreme aridity that occurred in much of the rest of the continent.

Given the mismatches between recent GCM simulations and paleoclimate records of H1 in

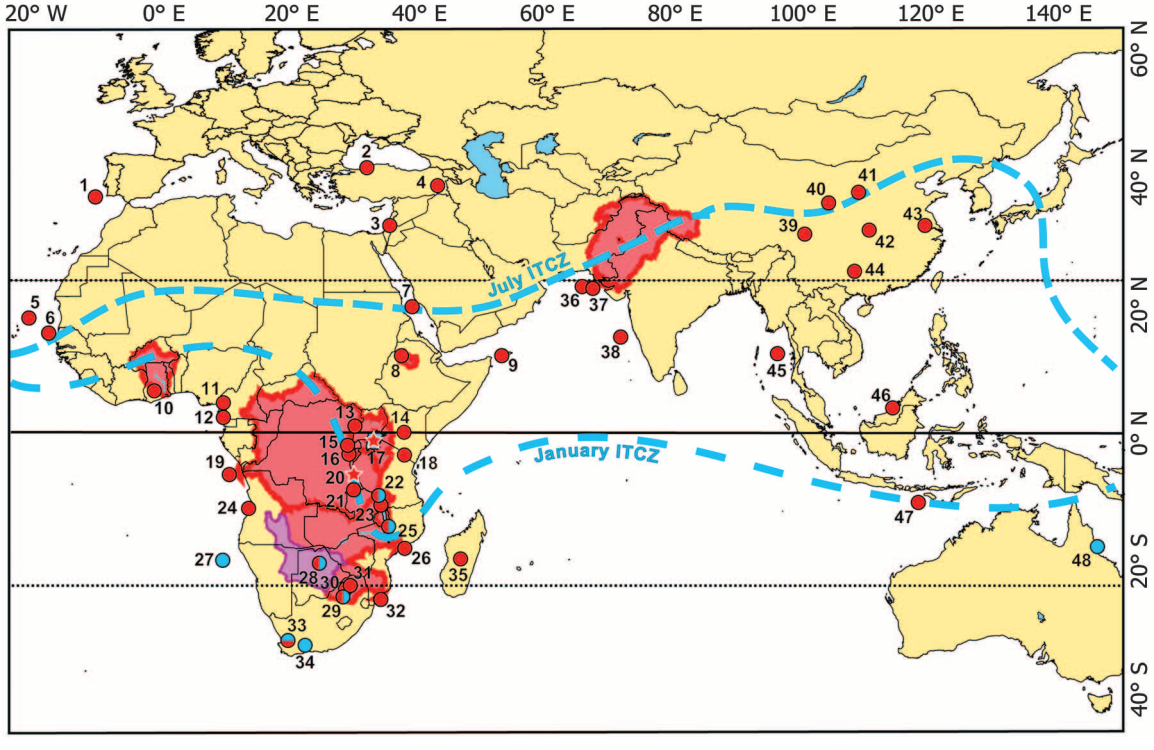

Fig. 1. Site map of records showing hydrological conditions during the 16- to 17-ka interval (details in table S3). Red dots, reduced precipitation-evaporation. Blue dots, increased precipitation-evaporation. Vertically divided red/blue dots indicate signals of uncertain climatic importance. Horizontally divided dots indicate a trend of progressively moister climates across HS-1. Only the specific study sites and some of the major watersheds are indicated; the full geographic area affected by the H1 megadrought is not completely colored in. For example, records from marine sites 5 and 6 reflect climatic conditions in much of northwestern Africa. Purple shading in the Kalahari region indicates wetter conditions of uncertain origin, timing, and/or geographic extent.

the Afro-Asian region, we suggest several possible causal mechanisms here. The occurrence of droughts throughout tropical Africa indicates that they most likely involved a reduction of convection and/or moisture content in the ITCZ, with or without a concurrent shift in its position. Surface warming in Lake Tanganyika during the driest interval of a 60,000-year sediment record (*18*) (Fig. 2D), for example, might indicate reduced evaporative cooling and upwelling linked to a weakening of atmospheric circulation over East Africa during H1; a severe reduction of summer monsoon wind activity was also registered in the Arabian Sea then (*8*). It has been hypothesized elsewhere that the southern limb of the tropical Hadley circulation system weakened during the longer HS-1 interval (*3*), which would also be consistent with the paleoclimate records indicating drought in equatorial and southern Africa.

Cooler SSTs in the SE Atlantic and Indian oceans also represent plausible mechanisms for the inferred reductions of tropical rainfall because lower SSTs would tend to reduce the evaporative moisture content of the ITCZ. Cooling along the West African coast likely contributed to summer monsoon failure there (*5*, *27*), and low SSTs in the western Indian Ocean (*28*) may likewise have contributed to aridity over eastern Africa. Conditions elsewhere along the margins of the Indian Ocean basin during H1 probably made SST cooling particularly widespread there as well. Stronger upwelling in the Southern Ocean may have cooled the southern margins of the Indian Ocean (*29*) and deflected cold, eastward-flowing water masses equatorward. Additionally, at that time much of today's warm Pacific through-flow was blocked by land masses in the Indonesian region due to a sea level low stand, thereby reducing Pacific heat inputs into the area, and reduced SSTs in much of the northern Indian Ocean (*8*, *21*) might have resulted from cooling by strong, south-trending winter monsoon winds over land masses that were concurrently chilled by conditions upwind in the Mediterranean and North Atlantic (*3*).

More than half of all humanity is strongly influenced by Afro-Asian rainfall systems today, and anatomically modern humans evolved under their influence, yet the mechanisms behind precipitation variability in these regions remain relatively poorly understood and difficult to model. Furthermore, the unusual intensity and exceptionally broad geographic distribution of the H1 megadrought have not yet been widely recognized. The records presented here show that it was one of the most intense and extensive tropical dry periods of the past 50,000 years or more (Figs. 1 and 2), spanning roughly 60 latitudinal degrees, virtually all of southern Asia, and most of the African continent, and that it must have involved a systemic, as yet unexplained weakening of regional rainfall systems in addition to southward displacement of the ITCZ. Whatever its exact cause, such a catastrophic drought would have had powerful effects on Paleolithic cultures. For example, the desiccations of Lakes Tana and Victoria reorganized the distribution of wet and arid-environment resources in the region, Middle Eastern drying would have hindered overland migrations into or out of Africa, and aridity around this time period likely contributed to major reductions in human populations in southern Asia (*30*).

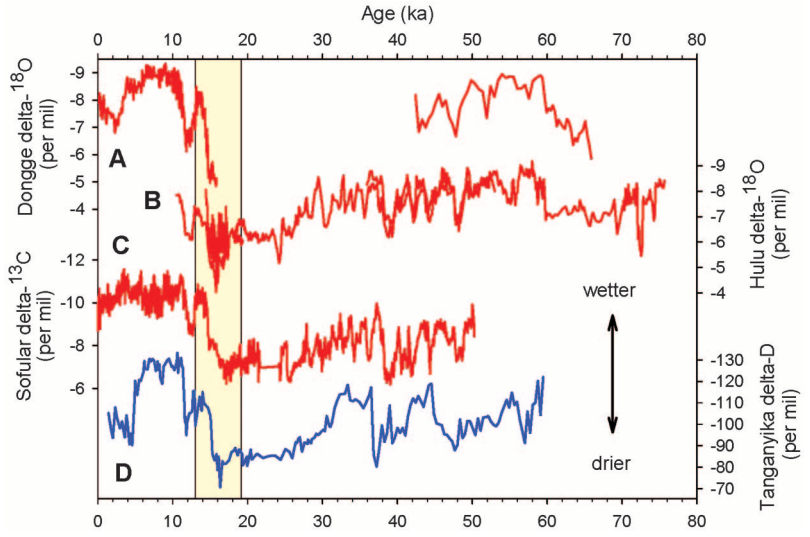

Fig. 2. Examples of terrestrial paleohydrological records in which the H1 signal was among the most intense of the past 50,000 years or more. (**A**) Dongge Cave, China, speleothem $\delta^{18}O$ (*9*). (**B**) Hulu Cave, China, speleothem $\delta^{18}O$, composite time series (*10*). (**C**) Sofular Cave, Turkey, speleothem $\delta^{18}O$ (*11*). (**D**) Lake Tanganyika, East Africa, δD (*18*). Although these records do not mean that all intervening sites necessarily experienced uniquely intense drought during H1, they do establish that the pattern was widely distributed, spanning southern Asia and extending south of the equator in East Africa. Colored column represents the 13- to 19-ka time period illustrated in Fig. 3.

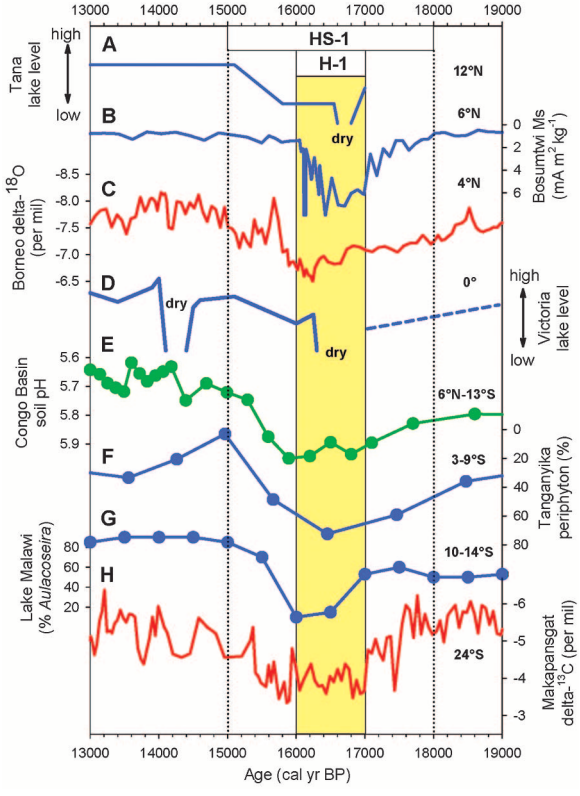

Fig. 3. Paleoclimatic records of the 13- to 19-ka interval from Africa and Borneo, ordered from north to south (latitude on right for each site). (**A**) Lake Tana, Ethiopia, relative level, no units [as in (*6*)]. (**B**) Lake Bosumtwi magnetic mineral concentration (*13*). (**C**) Borneo speleothem, $\delta^{18}O$ series (*16*). (**D**) Lake Victoria relative lake level (this study),. (**E**) Congo basin soil pH (*15*). (**F**) Lake Tanganyika percentage of periphytic diatoms (inverted; this study). (**G**) Lake Malawi *Aulacoseira nyassensis* with lower percentage indicating less windy and/or drier conditions [as in (*20*)]. (**H**) Stalagmite T7 from Cold Air Cave, $\delta^{13}C$ series (*31*). Brown bar, approximate H1 interval. Dotted lines bracket the approximate HS-1 interval. All time series are arranged with drying trends oriented downward.

References and Notes

1. L. C. Peterson, G. H. Haug, K. A. Hughen, U. Röhl, *Science* **290**, 1947 (2000).
2. M. Kageyama *et al.*, *Clim. Past* **5**, 551 (2009).
3. G. H. Denton *et al.*, *Science* **328**, 1652 (2010).
4. D. S. G. Thomas, R. Bailey, P. A. Shaw, J. A. Durcan, J. S. Singarayer, *Quat. Sci. Rev.* **28**, 526 (2009).

5. S. Mulitza *et al.*, *Paleoceanography* **23**, PA4206 (2008).
6. H. F. Lamb *et al.*, *Quat. Sci. Rev.* **26**, 287 (2007).
7. W. S. Broecker, D. Peteet, I. Hajdas, J. Lin, E. Clark, *Quat. Res.* **50**, 12 (1998).
8. H. Rashid, B. P. Flower, R. Z. Poore, T. M. Quinn, *Quat. Sci. Rev.* **26**, 2586 (2007).
9. D. Yuan *et al.*, *Science* **304**, 575 (2004).
10. Y. J. Wang *et al.*, *Science* **294**, 2345 (2001).
11. D. Fleitmann *et al.*, *Geophys. Res. Lett.* **36**, L19707 (2009).
12. D. Verschuren *et al.*; CHALLACEA project members, *Nature* **462**, 637 (2009).
13. J. A. Peck *et al.*, *Palaeogeogr. Palaeoclimatol. Palaeoecol.* **215**, 37 (2004).
14. S. Weldeab, D. W. Lea, R. R. Schneider, N. Andersen, *Science* **316**, 1303 (2007).
15. J. W. H. Weijers, E. Schefuss, S. Schouten, J. S. Sinninghe Damsté, *Science* **315**, 1701 (2007).
16. J. W. Partin, K. M. Cobb, J. F. Adkins, B. Clark, D. P. Fernandez, *Nature* **449**, 452 (2007).
17. Materials and methods are available as supporting material on *Science* Online.
18. J. E. Tierney *et al.*, *Science* **322**, 252 (2008).
19. E. Bard, F. Rostek, J.-L. Turon, S. Gendreau, *Science* **289**, 1321 (2000).
20. F. Gasse, P. Barker, T. C. Johnson, in *The East African Great Lakes: Limnology, Palaeoclimatology and Biodiversity,* E. O. Odada, D. O. Olago, Eds. (Kluwer Academic Publishers, Dordrecht, 2002), pp. 393-414.
21. L. Dupont, T. Caley, B. Malaize, J. Girardeau, *Geophys. Res. Abstr.* **12**, EGU2010-3892 (2010).
22. Y. Wang, T. Larsen, N. Andersen, T. Blanz, R. Schneider, *Geophys. Res. Abstr.* **12**, EGU2010-11360 (2010).
23. B. M. Chase, M. E. Meadows, *Earth Sci. Rev.* **84**, 103 (2007).
24. B. M. Chase *et al.*, *Geology* **39**, 19 (2010).
25. S. L. Burrough, D. S. G. Thomas, J. S. Singarayer, *Earth Sci. Rev.* **96**, 313 (2009).
26. J.-B. W. Stuut *et al.*, *Mar. Geol.* **180**, 221 (2002).
27. L. M. Dupont, H. Behling, J. H. Kim, *Clim. Past* **4**, 107 (2008).
28. E. Bard, F. Rostek, C. Sonzogni, *Nature* **385**, 707 (1997).
29. R. F. Anderson *et al.*, *Science* **323**, 1443 (2009).
30. S. Kumar *et al.*, *BMC Evol. Biol.* **8**, 230 (2008).
31. K. Holmgren *et al.*, *Quat. Sci. Rev.* **22**, 2311 (2003).
32. This study was supported by National Science Foundation grant EAR-0822922 (P2C2). F.S.R.P. has been supported by the Norwegian Research Council through the Decadal to Century-Scale Variability in East Asia Climate (DecCen) and Arctic Records of Climate Change (ARCTREC) projects. Sediment core samples were provided by D. Livingstone, T. Johnson, and C. Scholz.

Supporting Online Material

www.sciencemag.org/cgi/content/full/science.1198322/DC1
Materials and Methods
SOM Text
Figs. S1 and S2
Tables S1 to S3
References

27 September 2010; accepted 2 February 2011
Published online 24 February 2011;
10.1126/science.1198322

Complex Multicolor Tilings and Critical Phenomena in Tetraphilic Liquid Crystals

Xiangbing Zeng,[1] Robert Kieffer,[2] Benjamin Glettner,[2] Constance Nürnberger,[2] Feng Liu,[1] Karsten Pelz,[3] Marko Prehm,[3] Ute Baumeister,[3] Harald Hahn,[4] Heinrich Lang,[4] Gillian A. Gehring,[5] Christa H. M. Weber,[5] Jamie K. Hobbs,[5] Carsten Tschierske,[2]* Goran Ungar[1,6]*

T-shaped molecules with a rod-like aromatic core and a flexible side chain form liquid crystal honeycombs with aromatic cell walls and a cell interior filled with the side chains. Here, we show how the addition of a second chain, incompatible with the first (X-shaped molecules), can form honeycombs with highly complex tiling patterns, with cells of up to five different compositions ("colors") and polygonal shapes. The complexity is caused by the inability of the side chains to separate cleanly because of geometric frustration. Furthermore, a thermoreversible transition was observed between a multicolor (phase-separated) and a single-color (mixed) honeycomb phase. This is analogous to the Curie transition in simple and frustrated ferro- and antiferromagnets; here spin flips are replaced by 180° reorientations of the molecules.

Solid-state materials, particularly those performing useful functions, often have framework or cellular structures on the nanoscale (*1*). For example, crystalline zeolites (*2*) used in ion exchange or catalysis have frameworks whose shapes are determined by the covalent bond lengths and angles that tolerate little change. Each solid-state framework structure is specific to the individual compound. In contrast, in soft matter such as lyotropic liquid crystals (for example, surfactant-water systems) (*3*) or diblock copolymers (*4*), as well as in many biological systems, the shapes of the frameworks are determined primarily by the curvature of the interface between the two incompatible liquids (*5*). Hence they form a limited range of closed- or open-cell structures, typically micellar cubic or hexagonal (*3*). Liquid crystal (LC)–forming T-shaped block molecules bearing three types of mutually incompatible groups (triphilic) can be said to fall between those two extreme categories. Their self-assembly is governed by principles more general than those of crystals, yet the number of known framework LC structure types exceeds the number found in all lyotropics. Here we describe how the addition of a fourth incompatible group substantially broadens the range of cellular LC morphologies.

Among the many LC phases of the T-shaped compounds are a series of honeycombs (Fig. 1, A to C) (*6*, *7*). The aromatic rod-like cores (II in Fig. 1D) form cell walls connected at the "seams" by terminal hydrogen-bonding groups (I), typically glycerol (*7*). The honeycomb cells of polygonal cross-section and infinite length are filled by the fluid lateral chains (III). Depending on the ratio of the cubic root of the volume of III to the length of II, cells ranging from triangular to hexagonal were obtained (Fig. 1, A to C) (*6*, *7*). Projected on an Euclidian plane (*8*), most observed honeycombs are Archimedean tilings (all vertices are equal) or their duals (tile centers are replaced by vertices) (*6*).

The recent example of kagome LC tiling (*9*), supported by simulation (*9*, *10*), hints at the potential for substantial expansion of the range of honeycomb structures using X-shaped molecules bearing two different side chains (Fig. 1E). We prepared tetraphilic X-shaped LC compounds (Fig. 2) consisting of a terphenyl- (compounds **A**) or a larger oligo(phenyleneethinylene)-based (compounds **B**) rigid rod core (II in Fig. 1) with a glycerol group at each end (I), with two different types of flexible hydrophobic chains attached to either side of the rod-like core (III and IV) [for analytical details, see the supporting online material (SOM) text, section S1). III is a highly branched carbosilane-based hydrocarbon chain (Si chain), and IV is a semiperfluorinated chain (F chain). The chain volume to molecular core length ratios were chosen such (*7*) that triangular or square cells were expected in compounds **B** and hexagonal cells were expected in **A.**

Complete segregation of the side chains of X-shaped molecules into different columns, resulting in two-color tilings (Fig. 1, F and G), should be possible for triangular and square cells, where "color" refers to the composition of the honeycomb cell interior. However, such complete segregation is frustrated for hexagonal cells, where some mixing of Si and F chains cannot be avoided. This is illustrated in Fig. 1H: among the three molecules sharing a node, at least one F chain will be mixed with a Si chain. Two uniform colorings of the partially phase-separated hexagonal structure are possible, one three-color [*p3m*1 symmetry (Fig. 1I)] and the other two-color [*p6mm* (Fig. 1J)].

[1]Department of Materials Science and Engineering, University of Sheffield, Mappin Street, Sheffield S1 3JD, UK. [2]Institute of Chemistry, Organic Chemistry, Martin-Luther-University Halle-Wittenberg, Kurt-Mothes-Strasse 2, D-06120 Halle, Germany. [3]Institute of Chemistry, Physical Chemistry, Martin-Luther-University Halle-Wittenberg, Van-Danckelmann-Platz 4, D-06120 Halle, Germany. [4]Institute of Inorganic Chemistry, Technische Universität Chemnitz, Strasse der Nationen 62, 09111 Chemnitz, Germany. [5]Department of Physics and Astronomy, University of Sheffield, Hicks Building, Sheffield S3 7RH, UK. [6]World Class University Program of Chemical Convergence for Energy & Environment, School of Chemical and Biological Engineering, Seoul National University, Seoul, Korea.

*To whom correspondence should be addressed. E-mail: g.ungar@shef.ac.uk (G.U.); carsten.tschierske@chemie.uni-halle.de (C.T.)